Scientific Research Publishing

Materials Sciences and Applications, 2025, 16(3), 107-120
https://www.scirp.org/journal/msa
ISSN Online: 2153-1188
ISSN Print: 2153-117X

Electrochemical Corrosion Behaviour of Duplex Stainless Steels in Simulated Body Fluids

Francesco Rosalbino*, Giorgio Scavino, Graziano Ubvertalli

Dipartimento di Scienza dei Materiali e Ingegneria Chimica (DICHI), Politecnico di Torino, Torino, Italy
Email: *francesco.rosalbino@polito.it

How to cite this paper: Rosalbino, F., Scavino, G. and Ubvertalli, G. (2025) Electrochemical Corrosion Behaviour of Duplex Stainless Steels in Simulated Body Fluids. *Materials Sciences and Applications*, **16**, 107-120.
https://doi.org/10.4236/msa.2025.163006

Received: December 25, 2024
Accepted: March 4, 2025
Published: March 7, 2025

Abstract

The electrochemical behaviour of three duplex stainless steels, (SAF 2101, SAF 2304, SAF 2205) was investigated. Open circuit potential, E_{OC}, measurements, and electrochemical impedance spectroscopy (EIS) were employed both in phosphate-buffered saline solution (PBS, pH = 7.2) and in PBS simulating in vitro inflammatory conditions (PBS + H_2O_2, pH = 5.0). It has been established that the tendency of the investigated steel materials towards corrosion decreases in the following order: SAF 2101 < SAF 2304 < SAF 2205 in both aggressive environments. The superior corrosion resistance exhibited by SAF 2205 is ascribed to the formation of a passive film with enhanced protective effectiveness than the one formed on SAF 2101 and SAF 2304, and this improvement is ascribed to a synergistic effect of Mo + N owing to the high molybdenum content in the alloy.

Keywords

Duplex Stainless Steels, Corrosion Resistance, Phosphate Buffer Solution, Open Circuit Potential, Electrochemical Impedance Spectroscopy (EIS)

1. Introduction

Owing to its low cost and ease of formability in combination with adequate mechanical properties and relatively high corrosion resistance, AISI 316L stainless steel is one of the most commercially available biomaterials for orthopedic and dental implant manufacturing [1]-[3]. However, 316L can be susceptible to some forms of localized corrosion such as pitting and crevice corrosion depending on the environment. Body fluids represent a significantly aggressive media to the metallic materials, and interactions between metallic implants and the surrounding tissue have high importance. Despite the chemical composition of body fluids is quite complex, the three most significant parameters regarding their corrosiveness

are the presence of chloride ions, the concentration of the dissolved oxygen and pH levels. Most body fluids have a pH of 7.4, a temperature around 37˚C and a chloride concentration of around 0.9% NaCl. According to these parameters, body fluids appear to be slightly less aggressive than seawater [2]. Moreover, immediately after implantation, an inflammatory reaction can occur in response to the presence of the device. In such a case, fibrin and chloride ions surround the metallic biomaterial, with a consequent decrease in the local pH [4]. Acidification has a detrimental effect on the stability of the passive regime [5] [6]. Due to the relatively high nickel content (usually 10%) in the composition of AISI 316L, implant dissolution and subsequent release of metallic ions in the tissue can cause adverse, toxic, or carcinogenic reactions and high biological risks for the patients [1]-[3].

Duplex stainless steels (DSS) have a structure consisting of approximately equal amounts of ferrite and austenite and are characterized by high mechanical strength, excellent corrosion resistance, and good weldability, which led to their widespread use in oil, chemistry, petrochemical, and food industries and occasionally in the medical industry [7]. DSS have high localized corrosion resistance which can be compared with the titanium alloys, due to its passive surface film, which is a consequence of the high percentage of chromium in the alloy, enhanced by the synergistic effect of alloying elements such as nitrogen and molybdenum. Results in several published papers dealing with the use of DSS in orthopedics and orthodontic applications, including *in vitro* and *in vivo* studies, have shown similar biocompatibility with AISI 316L [8]-[10]. The replacement of AISI 316L with DSS in orthodontic treatments reduces costs and nickel hypersensitivity in patients [10].

With the aim of assessing the potential use of DSS as a biomaterial, the present work investigates the corrosion behaviour of three duplex stainless steels (SAF 2101, SAF 2304, SAF 2205), characterized by a lower Ni content compared to AISI 316L, during exposure to phosphate-buffer physiological solution (PBS) and PBS containing H_2O_2 (titrated to pH = 5.0) simulating in vitro inflammatory conditions. The study was carried out using open circuit potential and electrochemical impedance spectroscopy techniques.

2. Experimental Details

Table 1. Chemical composition (*wt.%*) of investigated duplex stainless steels.

Alloys	Cr	Ni	Mn	Si	C	Mo	N
SAF 2101	21.13	1.19	5.72	0.29	0.027	0.30	0.21
SAF 2205	22.21	5.45	1.52	0.33	0.013	3.10	0.18
SAF 2304	22.92	4.20	1.45	0.21	0.011	0.30	0.10

Electrochemical measurements were performed on three different duplex stainless steels (SAF 2101, SAF 2304, SAF 2205, supplied by Outokumpu) with the

chemical compositions (*wt.*%) reported in Table 1.

The test specimens were cut into discs of 15 mm diameter. The samples were ground with a sequence of 400 - 4000 grit emery paper and subsequently polished with alumina suspension to attain mirror-appearance, washed with Milli-Q de-ionized water (18.2 MΩ), ultrasonically cleaned and degreased in ethanol, and dried in air. Test specimens were embedded in a Teflon PAR holder and employed as the working electrode (WE). The reference electrode (RE) was a saturated calomel electrode (SCE, 0.242 V *vs.* SHE) and the counter electrode (CE) was a large platinum sheet. All the potentials described in the text are relative to the SCE, unless stated differently. A three-electrode flat KO2354 PAR corrosion cell (volume 0.25 L) was used and the test specimen employed as a WE was exposed to the aggressive environment with an area of 1 cm^2. Electrochemical measurements were performed for all specimens in two different aggressive environments:

1) phosphate-buffer saline solution (PBS: 8.0 g/L NaCl, 0.2 g/L KCl, 1.42 g/L Na_2HPO_4, 0.24 g/L KH_2PO_4, pH = 7.2 to simulate normal physiological conditions).

2) 150 mM H_2O_2 solution in PBS titrated to pH = 5.0 with HCl, to simulate inflammatory conditions [11] [12].

The aggressive media were naturally aerated and the experiments were conducted without stirring. The temperature was maintained at 37 ± 1˚C using a thermostatic bath. Electrochemical measurements were performed using a conventional three-electrode glass cell with a large platinum sheet and a saturated calomel electrode (SCE) serving as the counter and the reference electrodes, respectively.

Open circuit potential, E_{OC}, was measured with respect to the SCE every 60 s for a period of 2 h.

Electrochemical impedance spectroscopy (EIS) measurements were carried out at open circuit potential using an EG&G PAR system Model 2263 driven by a computer. The impedance spectra were acquired in the frequency range from 100 kHz to 10 mHz with a perturbation signal of 10 mV at seven points per decade. EIS plots were obtained after 2 h exposure to the test solution. Experimental data were stored in the computer and processed according to the EQUIVCRT program (B. A. Boukamp, University of Twente).

3. Results

3.1. PBS Solution

Figure 1 reports the open circuit potential, E_{OC}, variations vs. exposure time of the test samples in PBS for a period of 2 h. The E_{OC} is a characteristic value for each individual electrochemical system and arises as a result of structural changes that occur due to the anodic and cathodic reactions at the electrode/solution phase boundary [1]. The time profiles of E_{OC} obtained for the DSS under study are quite similar. As can be seen, the open circuit potential changes quickly towards more positive values during the first 1000 seconds. After that, E_{OC} changes more slowly

until it reaches a quasi-stationary value at 1 h, not changing significantly after that. This fact indicates that all the test samples undergo spontaneous passivation due to the formation of an oxide film passivating the metallic surface, in the PBS solution. The initial increase of E_{OC} is related to the thickening of the oxide film improving its corrosion protection ability [13] [14]. On the other hand, the observed stabilization of E_{OC} is ascribed to the reaching of the passive film limiting protective capacity [15]. The established E_{OC} value depends on the chemical composition of the DSS and after 2 h exposure to PBS solution is: 14.23 mV for SAF 2101, 63.90 mV for SAF 2304, and 114.65 mV for SAF 2205.

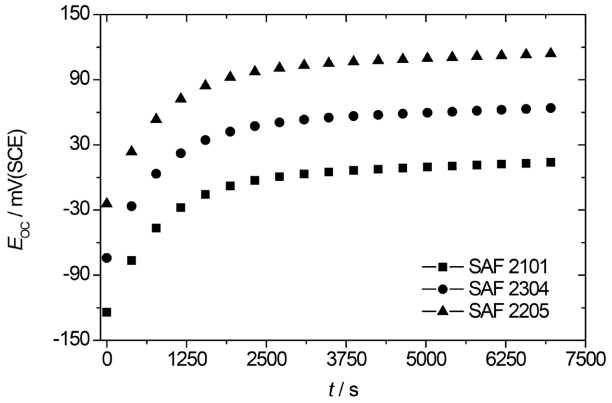

Figure 1. Corrosion potential vs. time profile for the investigated duplex stainless steels after 2 h exposure to PBS solution, pH = 7.4.

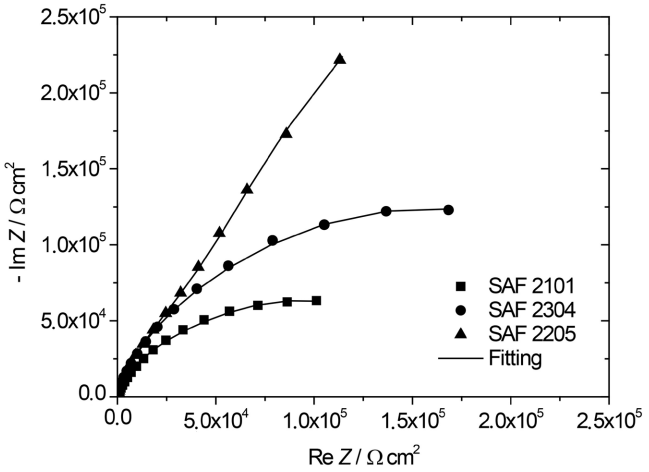

Figure 2. Representative Nyquist diagrams of duplex stainless steels after 2 h exposure to PBS solution, pH = 7.4.

The established E_{OC} value represents the balance between the formation and dissolution of the oxide film on the sample surface during the exposure time to the aggressive environment [1] [16]. Therefore, SAF 2205 with the highest E_{OC} value is the most stable material under spontaneous corrosion conditions. Similar behavior was observed for steel alloy both in PBS solution and in other corrosive environments of the human body [17].

Figure 2 displays the EIS spectra, in the form of Nyquist diagrams, of the three duplex stainless steels at open circuit potential, after 2 h exposure to PBS at 37˚C. All Nyquist diagrams present depressed and incomplete capacitive semicircles, the highest impedance values being measured for SAF 2205 suggesting a highly stable passive film on this alloy in the test environment.

The impedance spectra obtained have been interpreted in terms of an equivalent circuit, with the circuit elements representing electrochemical properties of the alloy and its surface oxide film. Figure 3 reports the equivalent circuit employed for fitting the spectra obtained for the investigated materials. This model is commonly proposed to mimic passive film with a duplex nature formed on stainless steels in simulated physiological environments [1] [18] [19]. It is known that that the oxide film grown at the surface of stainless steels presents a two-layer structure and consists of an inner compact film, *i.e.*, barrier film, and an outer porous film. Generally, the inner barrier layer exhibits a very high impedance, while the outer porous layer shows a significantly lower impedance [18] [20]-[22].

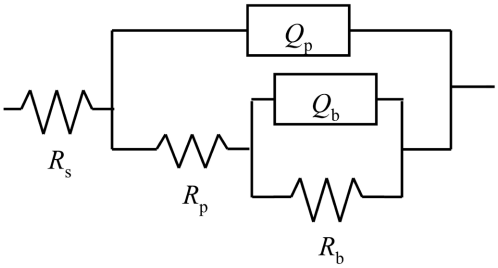

Figure 3. Equivalent electrical circuit model used for the interpretation of impedance spectra.

The equivalent circuit reported in Figure 3 consists of the electrolyte resistance, R_s, connected in series with two time constants: R_s (Q_p R_p) (Q_b R_b). The first time constant, (Q_p R_p), describes the properties of the outer part of the oxide film, where R_p and Q_p represent the resistance and capacitance, respectively, of the porous layer with the electrolyte inside the pores. The second time constant, (Q_b R_b), describes the properties of the compact, inner part of the oxide film, where R_b and Q_b represent the resistance and capacitance, respectively, of the barrier layer.

A constant phase element, CPE, was used for fitting the impedance spectra instead of a pure capacitance owing to the non-ideal capacitive response due to the distributed relaxation feature of the oxide film. The impedance of the CPE is given by:

$$Z_{\mathrm{CPE}} = \left[Y_0 \left(j \right) \omega^n \right]^{-1} \tag{1}$$

Where Y_0 is a constant, is the angular frequency and $1 \le n \le 1$. The value of n seems to be associated with the non-uniform distribution of current as a result of roughness and surface defects [23].

Analysis of the EIS spectra in terms of the equivalent circuit shown in Figure 3 allows the parameters Q_p, Q_b and R_p, R_b to be determined, and their values are

reported in Table 2. The agreement between experimental and simulated data indicates that the experimental impedance spectra are well fitted to the proposed equivalent circuit. The fitting quality was evaluated by chi-squared (χ^2) values of about 10^{-4}, with a relative error less than 5%. On the Nyquist plots in Figure 2, the experimental data are shown as individual points, while the fitted spectra are presented as continuous lines.

Table 2. Electrical parameters of equivalent circuit obtained by fitting the experimental results of EIS for investigated DSS in PBS solution at 37˚C.

Alloy	$Q_p \times 10^6$ ($\Omega^{-1}\cdot s^n\cdot cm^{-2}$)	n_p	R_p ($\Omega\cdot cm^2$)	$Q_b \times 10^6$ ($\Omega^{-1}\cdot s^n\cdot cm^{-2}$)	n_b	R_b ($\Omega\cdot cm^2$)
SAF 2101	130.87	0.94	$1.54 \cdot 10^3$	254.12	0.96	$1.71 \cdot 10^5$
SAF 2205	93.05	0.96	$4.68 \cdot 10^3$	196.77	0.98	$9.69 \cdot 10^5$
SAF 2304	112.26	0.95	$2.75 \cdot 10^3$	226.33	0.97	$3.02 \cdot 10^5$

Generally, the results reveal that the layer resistances of the passive film, R_p and R_b, are always in the order of $k\Omega\cdot cm^2$. However, for all steel samples, the resistance of the inner barrier layer, R_b, is significantly higher than the resistance of the outer porous layer, R_p. Moreover, the capacitance of the inner barrier layer ($n_b \approx 1$, $Q_b \approx C_b$) in all investigated materials is higher than the capacitance of the outer porous layer ($n_p \approx 1$, $Q_p \approx C_p$).

By considering the oxide film to act as a parallel plate dielectric, the passive layer thickness can be calculated according to [24]:

$$C = \varepsilon\varepsilon_0 A d^{-1} \tag{2}$$

Where ε is the dielectric constant of the oxide, ε_0 the vacuum permittivity, A the geometric area and d is the thickness. Since the capacitance, C values can be extracted from the CPE parameter, Q using [25]:

$$C_p = \left(R_p^{1-n} Q_p\right)^{1/n} \tag{3}$$

$$C_b = \left(R_b^{1-n} Q_b\right)^{1/n} \tag{4}$$

The thickness of the oxide film formed on the studied stainless steels can be estimated. To that end, $\varepsilon = 15.6$ is assumed, which is the value for the oxide film formed on austenitic stainless steels [19] [22]. This value is reasonable because the dielectric constants of oxides formed on stainless steels are between 10 and 20 [26]. The thickness of the passive film grown on the investigated materials during exposure to PBS is reported in Table 3. Despite the thickness of the inner barrier and outer porous layers is in the order of magnitude nm, all steel samples exhibit an inner barrier layer significantly thinner than the outer porous layer. Based on the above results, the corrosion of tested duplex stainless steels is mainly prevented by a thin compact barrier layer of high resistance.

As can be seen in Table 2 and Table 3, the resistance of the barrier and porous part of the passive film increases in order: SAF 2101 < SAF 2304 < SAF 2205. In

the same order, the thickness of oxide films increases, *i.e.*, the corresponding capacities decrease, which indicates better protective properties of the surface film on 2205 DSS compared to other alloys.

Table 3. Barrier and porous layer thickness estimated from EIS results for investigated DSS in PBS solution at 37˚C.

Alloy	d_b (nm)	d_p (nm)
SAF 2101	5.08	11.29
SAF 2205	7.12	14.20
SAF 2304	6.33	12.55

3.2. PBS Solution + 150 mM H_2O_2

After implantation, an inflammatory reaction is initiated both in response to the invasive procedure and the physical presence of the device as a foreign body. This reaction results in the production of reactive oxygen species by macrophages, neutrophils and other inflammatory response cells [27], which enzymes in the body quickly destroy by catalyzing their conversion to hydrogen peroxide (H_2O_2) [28]. In addition to the local increased concentration of H_2O_2, neutrophils produce lactic acid leading to an acidic pH in the immediate implant environment. In order to simulate an inflammatory response, DSS specimens were immersed in a PBS solution titrated to pH = 5.0 with 150 mM H_2O_2. This environment exposes the investigated alloys to aggressive corrosive conditions compared to the specimens tested under normal physiological conditions where the initial pH of PBS was measured to be 7.2.

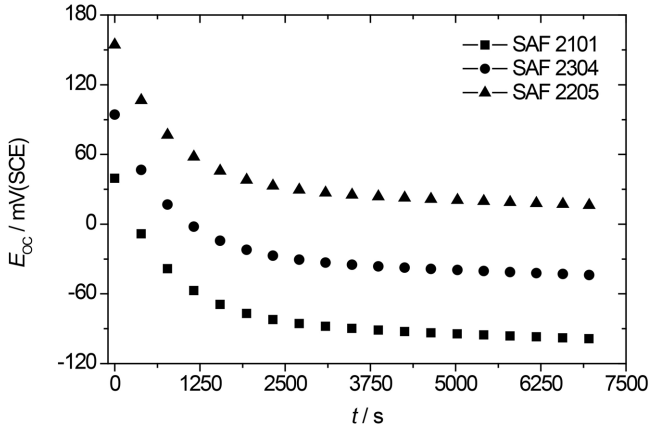

Figure 4. Corrosion potential vs. time profile for the investigated duplex stainless steels after 2 h exposure to PBS + H_2O_2 solution, pH = 5.0.

Figure 4 reports the evolution of the open-circuit potential, E_{OC}, of the investigated DSS as a function of exposure time to PBS containing 150 mM H_2O_2, pH = 5.0. As can be seen, at initial time points the inflammatory conditions shift E_{OC} to more positive values when compared to the normal conditions (**Figure 1**). After

that, the open-circuit potential changes towards more negative values over exposure time to the aggressive environment, suggesting dissolution of the oxide film and surface activation of the alloys. According to the Nernst equation, it is likely the acidic pH under inflammatory conditions contributes to the positive shift of E_{OC} observed at early time points of exposure. This observation is consistent with others who have reported electro-positive shift in 316L austenitic stainless steel when exposed to acidic solutions [4] [11] [29]. Likewise, the presence of H_2O_2 provides an additional species to be reduced in the electrolyte, further contributing to the positive values of E_{OC} measured at initial exposure times. Electro-positive shift in 316L E_{OC} when immersed in solutions containing H_2O_2 has also been previously reported [29] [30].

As reported in **Figure 4**, the open circuit potential of SAF 2205 stabilizes at less negative values compared to the other alloys. As a matter of fact, the value of E_{OC} after 2 h exposure to the aggressive environment is: −99.52 mV for SAF 2101, −43.32 mV for SAF 2304, and 16.13 mV for SAF 2205.

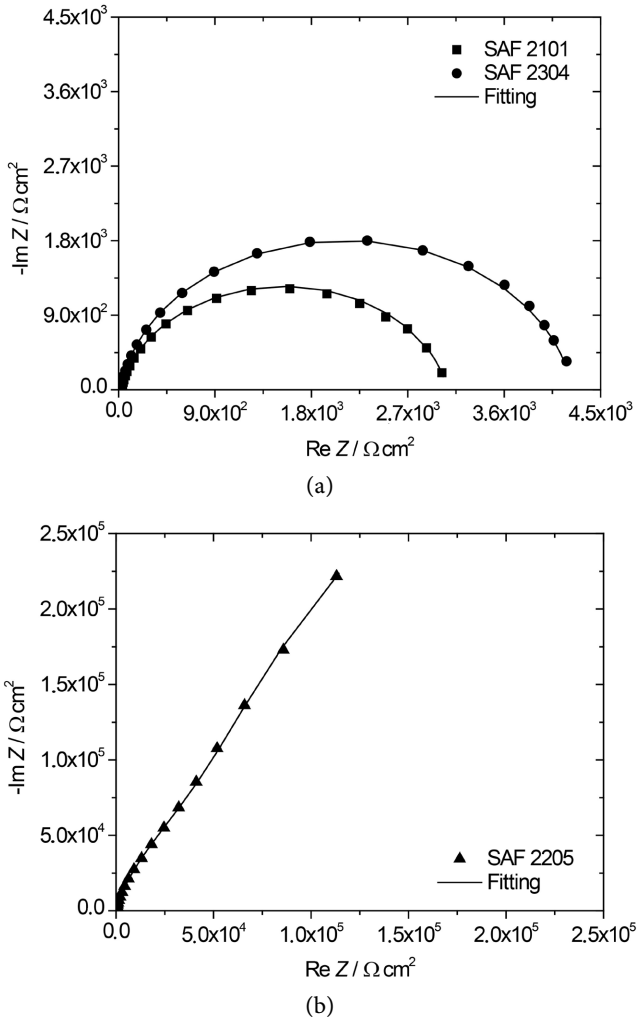

Figure 5. Representative Nyquist diagrams of duplex stainless steels after 2 h exposure to PBS + H_2O_2 solution, pH = 5.0.

Table 4. Electrical parameters of equivalent circuit obtained by fitting the experimental results of EIS for investigated DSS in PBS + 150 mM H_2O_2, pH = 5.0, at 37˚C.

Alloy	$Q_p \times 10^6$ ($\Omega^{-1}\cdot s^n\cdot cm^{-2}$)	n_p	R_p ($\Omega\cdot cm^2$)	$Q_b \times 10^6$ ($\Omega^{-1}\cdot s^n\cdot cm^{-2}$)	n_b	R_b ($\Omega\cdot cm^2$)
SAF 2101	155.37	0.92	2.06×10^2	277.49	0.94	2.84×10^3
SAF 2205	101.58	0.94	3.17×10^3	215.24	0.96	8.45×10^5
SAF 2304	129.41	0.93	4.03×10^2	248.63	0.95	3.97×10^3

This behaviour would indicate higher stability of the oxide film and consequently lower surface activation of 2205 alloy with respect to the other investigated materials.

In order to verify the results of E_{OC} measurements, EIS investigation was carried out. Figure 5 presents the impedance measurements traced over the frequency domain 0.01 Hz - 100 kHz at the stabilized E_{OC} after 2 h immersion, as Nyquist plots in PBS containing 150 mM H_2O_2, pH = 5.0. In this case, differences can be observed between the spectra which vary significantly between the tested materials. As a matter of fact, two different situations can be distinguished: 2101 and 2304 DSS exhibit lower impedance values with respect to the PBS alone; conversely, SAF 2205 show an impedance value similar to that obtained in PBS thus confirming better corrosion resistance of this alloy, in accordance with the study using open circuit potential measurements. The EIS spectra measured for the DSS under study could be satisfactorily fitted with the two-layer model reported in Figure 3. The fitting quality was evaluated by the chi-squared values, which were in the order of 10^{-4}. The values of fitted parameters of the equivalent circuit are listed in Table 4. As can be seen, SAF 2101 and SAF 2304 DSS display significantly lower R_b values, almost two order of magnitude smaller, compared to those obtained in PBS alone, indicating a thinning of the oxide passive film and, consequently, a remarkable decrease of corrosion resistance. Conversely, the R_b value of SAF 2205 is of the same order of magnitude as determined in PBS, suggesting that the passive film formed at the surface of this alloy is still able to protect the underlying metallic matrix even in a more aggressive environment such as PBS containing 150 mM H_2O_2, pH = 5.0.

4. Discussion

Since corrosion resistance of stainless steels is proportional to the content of alloying elements that enhance passive film stability and the absence of those that reduce it, the chemical composition plays a very important role in determining the stability and thickness of the passive film which forms at the surface of DSS under study (Table 1). Elements that enable passivation of the steel will enhance the protective properties of the oxide film (higher resistance and thickness, more compact structure).

It is well established that the passive film is described as a mixed oxyhydroxide layer composed mainly of chromium and iron, typically 1 - 3 nm thick. Chromium

and iron are usually found in their trivalent states, preferentially in the inner and outer parts of the passive film, respectively. For a sufficient chromium content in the alloy, preferential chromium oxidation and/or preferential iron dissolution in acidic media leads to a significant Cr (III) enrichment in the oxide layer, conferring to the passive film its protective nature [31]. The characteristic of the passive film as well as of the underlying metal strongly depends on the composition of the alloy. For Ni-bearing austenitic and duplex stainless steels, the selective oxidation of iron and chromium leads to a very low and often non-detectable amount of oxidized nickel in the passive film, while metallic nickel is enriched in the underlying metal [32]. For Mo-bearing ferritic, austenitic and duplex stainless steels, a small amount of oxidized molybdenum is detected. Mo (VI) is reported to be enriched in the surface region, while Mo (IV) distribution through the passive film is more homogeneous [33]. Nitrogen added to austenitic and duplex stainless steels can be enriched by anodic segregation during passivation, leading to the formation of a mixed-nitride phase either at the metal/oxide interface or incorporated in the passive film [34].

Moreover, it has been reported that the concurrent presence of nitrogen and a suitable molybdenum content in the alloy significantly increases the corrosion resistance of stainless steels because the passive film is more resistant to attack by aggressive ions due to the a synergistic effect of these elements [35]-[37]. The explanation for the mechanism behind can be generally summarized as follows:

a) optimizing the components of passive film: Kim [38] proposed that the content of corrosion resistant Cr_2O_3 in the passive film is improved after combined addition of N and Mo, which enhances the protection ability of passive film.

b) mutual promotion between NH_3/NH_4^+ and MoO_4^{2-}: Olsson [39] found that the NH_4^+ content at the surface of Mo-bearing duplex stainless steel is higher than that of Mo-free austenite, indicating that MoO_4^{2-} can promote the formation of NH_4^+. Loable *et al*. [40] proposed an interesting assumption that NH_3 and NH_4^+ in the passive film may in turn assist the formation of MoO_4^{2-}, which is an effective corrosion-inhibiting anion.

c) forming mixed nitride with high stability: Willenbruch, Clayton *et al*. [41] [42] proposed that for the N-bearing and Mo-bearing stainless steel, there would be mixed metal nitride of Ni and Mo (Ni_2Mo_3N) locating at the interface between matrix and passive film. Ni_2Mo_3N is more stable than Ni_3N and Mo_2N, thereby providing better protection for the steel matrix.

Based on the ideas presented, the influential role of Cr, Mo and N as active partners in forming a more stable passive film at the steel surface with good anticorrosive properties can be readily perceived by comparing the R_b values. As previously reported, the inner barrier layer resistance tends to be lower in PBS + H_2O_2 than in PBS, however R_b falls to very low values for SAF 2101 and SAF 2304 while SAF 2205 shows a R_b value over two orders of magnitude higher. The present results indicate that the surface oxide layer formed on SAF 2205 exhibits a higher degree of passivation and stability than the oxide film presents at the surface of SAF 2101 and SAF 2304 in both aggressive environments. Since the DSS under

investigation have comparable Cr contents (Table 1), the observed behaviour can be ascribed to a strengthening of the passive layer due to the synergetic effect of nitrogen and high content molybdenum (3.10%).

The enhanced protective properties of passive film present at the surface of SAF 2205, highlighted by the larger R_b values with respect to the other alloys, pointing out its higher corrosion resistance in solutions simulating the normal physiological environment or an inflammatory environment, in agreement with the results obtained from open-circuit potential measurements (Figure 1).

Further studies about properties investigation and surface analyses of SAF 2205 are planned aiming to a deeper understanding of the protective behavior of its passive oxide film. Besides, Tsai *et al.* [43] have reported the galvanic corrosion of DSS in aggressive environments, *i.e.*, in mixed H_2SO_4/HCl and HNO_3 solutions, due to the difference in the chemical composition between the ferritic and the austenitic phases. The galvanic corrosion of SAF 2205 was not considered in the present study; however, it is an interesting topic for future investigations, to assess the potential risk of galvanic corrosion between the ferrite and the austenite phases of SAF 2205 with respect to orthodontic or orthopedic applications.

5. Conclusions

The electrochemical corrosion behaviour of three duplex stainless steels, SAF 2101, SAF 2304, SAF 2205, has been characterized in PBS solution (pH = 7.2) and in PBS simulating in vitro inflammatory conditions (PBS + H_2O_2, pH = 5.0) in order to investigate their potential use as biomaterials. The alloys were tested by 2 h open-circuit potential, E_{OC}, and electrochemical impedance spectroscopy (EIS) measurements.

E_{OC} measurements performed in PBS solution indicated that all DSS undergo spontaneous passivation due to spontaneously formed oxide film passivating the metallic surface. However, SAF 2205 presents higher E_{OC} values, indicating that its passive film seems to exhibit better corrosion protection characteristics than the one formed on SAF 2101 and SAF 2304.

In simulated inflammatory conditions, EOC measurements show active behaviour in all the investigated alloys. However, a significant increase in stability of the passive oxide layer and consequently a decrease in surface activation is observed for SAF 2205.

The observed behaviour is confirmed by EIS measurements. In fact, SAF 2205 exhibits higher impedance values as compared with the other alloys, especially in PBS simulating in vitro inflammatory conditions.

The overall electrochemical data indicate a positive influence of alloy chemical composition on the corrosion behaviour of SAF 2205. The better corrosion resistance can be ascribed to a strengthening of the passive oxide film due to the simultaneous presence of nitrogen and high content molybdenum, thus enhancing its protective capability owing to the synergistic effect of these elements.

The corrosion characteristics of SAF 2205 suggest its suitability for orthodontic

or orthopedic applications, because the electrochemical stability of this alloy is directly associated with biocompatibility.

Conflicts of Interest

The authors declare no conflicts of interest regarding the publication of this paper.

References

[1] Gudić, S., Nagode, A., Šimic, K., Vrsalović, L. and Jozić, S. (2022) Corrosion Behaviour of Different Types of Stainless Steel in PBS Solution. *Sustainability*, **14**, Article 8935. https://doi.org/10.3390/su14148935

[2] Blackwood, D.J. (2003) Biomaterials: Past Successes and Future Problems. *Corrosion Reviews*, **21**, 97-124. https://doi.org/10.1515/CORRREV.2003.21.2-3.97

[3] Hansen, D. (2008) Metal Corrosion in the Human Body the Ultimate Biocorrosion Scenario. *The Electrochemical Society Interface*, **17**, 31-34. https://doi.org/10.1149/2.F04082IF

[4] Lopez, D.A., Duran, L. and Cere, S. (2001) Electrochemical Characterization of AISI 316L Stainless Steel in Contact with Simulated Body Fluid under Infection Conditions. *Journal of Materials Science*: *Materials in Medicine*, **19**, 2137-2144. https://doi.org/10.1007/s10856-007-3138-y

[5] Solar, R.J. (1979) Corrosion and Degradation of Implant Materials. American Society for Testing and Materials, 259.

[6] Marshall, P.J. and Burstein, G.T. (1983) The Effects of pH on the Repassivation of 304L Stainless Steel. *Corrosion Science*, **23**, 1219-1228. https://doi.org/10.1016/0010-938X(83)90049-5

[7] Köse, C., Kacar, R., Zorba, A.P., Bağirova, M., Abramor, E.S. and Allahverdiyev, A.M. (2018) Interactions between Fibroblast Cells and Laser Beam in AISI 2205 Duplex Stainless Steel. *Materials Science* (*Medžiagotyra*), **24**, 159-165. https://doi.org/10.5755/j01.ms.24.2.18006

[8] Beloti, M.M., Rollo, J.M.D.A., Itman Filho, A. and Rosa, A.L. (2004) *In Vitro* Biocompatibility of Duplex Stainless Steel with and without 0.2% Niobium. *Journal of Applied Biomaterials & Biomechanics*, **2**, 162-168.

[9] Kocijan, A. and Conradi, M. (2010) The Corrosion Behaviour of Austenitic and Duplex Stainless Steel in Artificial Body Fluids. *Materials and Technologies*, **44**, 21-24.

[10] Hammood, A.S., Noor, A.F. and Alkhafagy, M.T. (2017) Effect of Heat Tretament on Corrosion Behaviour of Duplex Stainless Steel in Orthodontic Applications. *Materials Research Express*, **4**, Article 126506. https://doi.org/10.1088/2053-1591/aa9c02

[11] Brooks, E.K., Brooks, R.P. and Ehrensberger, M.T. (2017) Effects of Simulated Inflammation on the Corrosion of 316L Stainless Steel. *Materials Science and Engineering*: *C*, **71**, 200-205. https://doi.org/10.1016/j.msec.2016.10.012

[12] Fonseca, C. and Barbosa, M.A. (2001) Corrosion Behaviour of Titanium in Biofluids Containing H_2O_2 Studied by Electrochemical Impedance Spectroscopy. *Corrosion Science*, **43**, 547-559. https://doi.org/10.1016/S0010-938X(00)00107-4

[13] Assis, S.L., Rogero, S.O., Antunes, R.A., Padilha, A.F. and Costa, I. (2005) A Comparative Study of the *In Vitro* Corrosion Behaviour and Cytotoxicity of a Superferritic Stainless Steel, a Ti-13Nb-13Zr Alloy, and an Austenitic Stainless Steel in Hank's Solution. *Journal of Biomedical Materials Research Part B*: *Applied Biomaterials*, **73B**, 109-116. https://doi.org/10.1002/jbm.b.30205

[14] Davies, J.R. (2000) Corrosion: Understanding the Basics. ASM Technical Books, 227. https://doi.org/10.31399/asm.tb.cub.9781627082501

[15] Yu, S.Y. and Scully, J.R. (1997) Corrosion and Passivity of Ti-13% Nb-13% Zr in Comparison to Other Biomedical Implant Alloys. *Corrosion*, **53**, 965-976. https://doi.org/10.5006/1.3290281

[16] Quin, P., Lui, Y., Sercombe, T.B., Li, Y., Zhang, C., Cao, C., Sun, H. and Zhang, L.C. (2018) Improved Corrosion Resistance on Selective Laser Melting Procedure Ti-5Cu Alloy after Heat Treatment. *ACS Biomaterials Science & Engineering*, **4**, 2633-2642. https://doi.org/10.1021/acsbiomaterials.8b00319

[17] El-Taib-Heakal, F., Shebata, O.S. and Tantawy, N.S. (2014) Integrity of Metallic Medical Implants in Physiological Solutions. *International Journal of Electrochemical Science*, **9**, 1986-2004. https://doi.org/10.1016/S1452-3981(23)07905-1

[18] Rondelli, G., Torricelli, P. and Giardino, M. (2005) *In Vitro* Corrosion Study by EIS of a Nickel-Free Stainless Steel for Orthopedic Applications. *Biomaterials*, **26**, 739-744. https://doi.org/10.1016/j.biomaterials.2004.03.012

[19] Tudose, A.E., Demetrescu, I., Golgovici, F. and Fulger, M. (2021) Oxidation Behaviour of an Austenitic Steel (Fe, Cr and Ni), the 310 H, in a Deaerated Supercritical Water System. *Metals*, **11**, Article 571. https://doi.org/10.3390/met11040571

[20] Antunes, A., De Oliveira, M.C.L. and Costa, I. (2012) Study of the Correlation Between Corrosion Resistance and Semi-Conducting Properties of the Passive Film of AISI 316L Stainless Steel in Physiological Solution. *Materials and Corrosion*, **63**, 586-592. https://doi.org/10.1002/maco.201006052

[21] Valero Vidal, C. and Igual Munoz, A. (2008) Electrochemical Characterization of Biomedical Alloys for Surgical Implants in Simulated Body Fluids. *Corrosion Science*, **50**, 1954-1961. https://doi.org/10.1016/j.corsci.2008.04.002

[22] Hakiki, N.E., Boudin, S., Rondot, B. and Da Cunha Belo, M. (1995) The Electronic Structure of Passive Films Formed on Stainless Steels. *Corrosion Science*, **37**, 1809-1822. https://doi.org/10.1016/0010-938X(95)00084-W

[23] Macdonald, J.R. (1987) Impedance Spectroscopy. John Wiley & Sons.

[24] Wegrelius, L., Falkenberg, F. and Olefjord, I. (1999) Passivation of Stainless Steels in Hydrochloric Acid. *Journal of the Electrochemical Society*, **146**, Article 1397. https://doi.org/10.1149/1.1391777

[25] Abreu, C.M., Cristobal, M.J., Losada, R., Novoa, X.R., Pena, G. and Perez, M.C. (2004) Comparative Study of Passive Films of Different Stainless Steels Developed on Alkaline Medium. *Electrochimica Acta*, **49**, 3049-3056. https://doi.org/10.1016/j.electacta.2004.01.064

[26] Boudalia, M., Guenbour, A., Bellaouchou, A., Fernandez-Domene, R.M. and Garcia-Anton, J. (2013) Corrosion Behaviour of a Highly Alloyed Austenitic Alloy UB6 in Contaminated Phosphoric Acid. *International Journal of Corrosion*, **20**, Article 363826. https://doi.org/10.1155/2013/363826

[27] Anderson, J.M., Rodriguez, A. and Chang, D.T. (2008) Foreign Body Reaction on Biomaterials. *Seminars in Immunology*, **20**, 86-100. https://doi.org/10.1016/j.smim.2007.11.004

[28] Babior, B., Kipnes, R. and Curnutte, J. (1973) The Production by Leukocytes of Superoxide, a Potential Bactericidal Agent. *Journal of Clinical Investigation*, **52**, 741-744. https://doi.org/10.1172/JCI107236

[29] Bennet, D. (1984) Effects of pH and Peroxide Addition on Corrosion of Type 316L Stainless Steel in Chloride Dioxide Bleaching Stage Washer Environment. *Corrosion*,

40, 1-5. https://doi.org/10.5006/1.3579290

[30] Bellanger, G. (1994) Effect of the Hydrogen Peroxide Formed in Tritiated Water on the Behaviour of 316L Stainless Steel. *Journal of Nuclear Materials*, **210**, 63-72. https://doi.org/10.1016/0022-3115(94)90223-2

[31] Gardin, E., Zanna, S., Seyoux, A., Allion-Maurer, A. and Marcus, P. (2018) Comparative Study of the Surface Oxide Films on Lean Duplex and Corresponding Single Phase Stainless Steels by XPS and ToF-SIMS. *Corrosion Science*, **143**, 403-413. https://doi.org/10.1016/j.corsci.2018.08.009

[32] Olefjord, I. and Wegrelius, L. (1990) Surface Analysis of Passive State. *Corrosion Science*, **31**, 89-98. https://doi.org/10.1016/0010-938X(90)90095-M

[33] De Vito, E. and Marcus, P. (1992) XPS Study of Passive Films Formed on Molybdenum-Implanted Austenitic Stainless Steels. *Surface and Interface Analysis*, **19**, 403-408. https://doi.org/10.1002/sia.740190175

[34] Olefjord, I. and Wegrelius, L. (1996) The Influence of Nitrogen on the Passivation of Stainless Steels. *Corrosion Science*, **38**, 1203-1220. https://doi.org/10.1016/0010-938X(96)00018-2

[35] Sedriks, A.J. (1986) Effects of Alloy Composition and Microstructure on the Passivity of Stainless Steels. *Corrosion*, **42**, 376-389. https://doi.org/10.5006/1.3584918

[36] Oh, K.-T., Kim, Y.-S., Park, Y.-S. and Kim, K.-N. (2004) Properties of Super Stainless Steels for Orthodontic Applications. *Journal of Biomedical Materials Research Part B*: *Applied Biomaterials*, **69B**, 183-194. https://doi.org/10.1002/jbm.b.30002

[37] Feng, H., Dai, J., Li, H., Cao, X., Zhu, H., Zhang, S., He, T., Jiang, Z. and Zhang, T. (2024) Visualizing and Quantifying the Influence of N-Mo Synergy on Corrosion Resistance of Stainless Steel by Dissolution-Diffusion-Deposition Model. *Corrosion Science*, **235**, Article 112162. https://doi.org/10.1016/j.corsci.2024.112162

[38] Kim, D. (1992) A Study of the Effect of Nitrogen and Molybdenum in the Corrosion Inhibition of Austenitic Stainless Steels. State University of New York.

[39] Olsson, C.O.A. (1995) The Influence of Nitrogen and Molybdenum on Passive Films Formed on the Austenoferritic Stainless Steel 2205 Studied by AES and XPS. *Corrosion Science*, **37**, 467-479. https://doi.org/10.1016/0010-938X(94)00148-Y

[40] Loable, C., Vicosa, I.N., Mesquita, T.J., Mantel, M., Nogueira, R.P., Brthonnè, G., Chauveau, E. and Roche, V. (2017) Synergy between Molybdenum and Nitrogen on the Pitting Corrosion and Passive Film Resistance of Austenitic Stainless Steels as a pH-Dependent Effect. *Materials Chemistry and Physics*, **186**, 237-245. https://doi.org/10.1016/j.matchemphys.2016.10.049

[41] Willenbruch, R.D., Clayton, C.R., Overslulzen, M., Kim, D. and Lu, Y. (1990) An XPS and Electrochemical Study of the Influence of Molybdenum and Nitrogen on the Passivity of Austenitic Stainless Steels. *Corrosion Science*, **31**, 179-190. https://doi.org/10.1016/0010-938X(90)90106-F

[42] Clayton, C.R., Halada, G.P. and Kearns, J.R. (1995) Passivity of High-Nitrogen Stainless Alloys: The Role Metal Oxyanions and Salt Films. *Materials Science and Engineering*: *A*, **198**, 135-144. https://doi.org/10.1016/0921-5093(95)80068-6

[43] Tsai, W.-T. and Chen, J.-R. (2007) Galvanic Corrosion between the Constituent Phases in Duplex Stainless Steels. *Corrosion Science*, **49**, 3659-3668. https://doi.org/10.1016/j.corsci.2007.03.035